SAND2006-0081 C

STRENGTH TESTING AND FRACTOGRAPHY OF MEMS MATERIALS

S. J. Glass, D. A. LaVan, T. E. Buchheit, and K. Jackson
Sandia National Labs, Albuquerque, NM 87185

ABSTRACT

The safe, secure, and reliable application of microelectromechanical systems (MEMS) devices requires knowledge about the MEMS materials' strength distributions and strength-limiting flaws. Sandia has developed a microtensile testing technique that uses the lateral force capabilities of a computer-controlled Nanoindenter to quantify the strength distribution of MEMS materials such as silicon and amorphous diamond. The sample sizes reflect the critical dimensions and features typical of MEMS devices. Multilayer polysilicon made using Sandia's SUMMiT process was successfully tested using several generations of uniaxial tensile samples, 1.8 μm wide and 2.5 μm thick, with lengths from 15 to 1000 μm. The average strength for first-generation polysilicon samples was 2.2±0.4 GPa, with a Weibull modulus of 7. Fracture strengths fell into three strength levels that matched three observed failure modes. Samples fabricated with an improved design showed increased strengths of 4.3±0.6 GPa and a Weibull modulus of 8. Similar samples with a tungsten coating had a lower average strength of 2.7±0.6 GPa and a Weibull modulus of 5. Failure origin sizes were estimated to be 14-44 nm. Comparisons of failure stress based on predictions from fracture surface features gave good agreement with measured strengths. An average strength greater than 8 GPa was measured for similar-scale samples fabricated from amorphous diamond, a high-strength, wear-resistant candidate MEMS material.

BACKGROUND

The subject of this paper is the strength testing and fractography of microelectromechanical systems (MEMS) materials being developed and evaluated at Sandia National Laboratories. Fabrication of MEMS devices for a variety of applications, including optical switches and displays, micro-relays, accelerometers, gyroscopes, image correctors, print-heads, flow sensors, and medical devices, is currently of great interest. MEMS devices are also being considered for a number of applications where high reliability is critical, including micromotors and stronglink safety devices. MEMS are fabricated in a fashion similar to microelectronics of the integrated circuit (IC) industry, but at the end of the process, free standing structures are created by removing the surrounding oxide matrix.

Most MEMS devices are currently being made from polycrystalline silicon (polysilicon). Polysilicon is to date the most successful MEMS material because many conflicting requirements can be satisfied simultaneously. First, processing of the material is fully compatible with standard IC processing techniques. Second,

residual stresses and stress gradient can be reduced to near zero. Stress gradients cause out-of-plane warpage, but nearly flat structures can be achieved by careful attention to processing. Third, multiple levels of polysilicon can be deposited, allowing complex elements to be made. The layers are stacked on top of each other and separated by deposited oxide layers. Connections between layers of polysilicon are made by cuts in the oxide layers. Figure 1 shows a photo of a 24-bit lock to demonstrate the scale and complexity of the devices that are currently being fabricated using Sandia National Laboratories' Ultra-planar Multi-level MEMS Technology (SUMMiT) process.[1,2] Fourth, polysilicon as deposited by chemical vapor deposition is highly conformal, coating uniformly even under overhangs, enabling hubs, hinges, pin joints and flanges to be built. Fifth, polysilicon exhibits excellent mechanical properties such as creep resistance and fatigue. The strength of the material is high compared to typical levels of stress encountered by structural members in MEMS. Polysilicon can be manufactured with very low levels of impurities and very few mechanical defects.

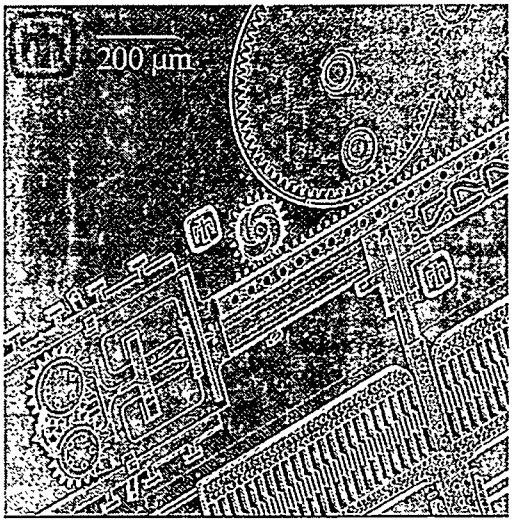

Fig. 1 A 24-bit lock made using Sandia's SUMMiT process. A display of several features including the 24-bit path, drive gears, anti-reversing gears, and meshing gears.

At Sandia National Laboratories we prototype advanced MEMS components with up to five levels of polysilicon. To enable motion of the structures, the encasing oxide is removed in a "release" etch of hydrofluoric acid, which removes the oxide, but not the polysilicon. If parts are transferred to water and then dried, they will adhere to the substrate because of capillary action resulting from the surface tension of water. "Dimples", locally recessed areas in the polysilicon, are created by a special mask in the processing sequence, to reduce the contact area of the structural material, as a geometrical method to reduce adhesion. However, dimples alone do not eliminate the adhesion problem. We are studying three other approaches to eliminate the adhesion problem during the release process. One approach is to dry parts in a supercritical CO_2 chamber. This results in structurally

DISCLAIMER

free devices, but surfaces remain hydrophilic and therefore susceptible to adhesion, friction and wear. A second approach is by solution coating devices with monolayer silane coupling agents. Again, free structures result, but the surfaces are now hydrophobic, and exhibit low adhesion and friction. However, monolayers can be removed by rubbing action. A third approach is to coat the silicon with a hard layer. We are investigating a selective tungsten coating that integrates well with our process flow. Tungsten-coated devices exhibit no wear. However, they are hydrophilic, and therefore remain susceptible to adhesion.

Several issues are of paramount importance in order to guarantee the reliability of polysilicon MEMS. Because the polysilicon surfaces are hydrophilic and therefore susceptible to water condensation, this often results in catastrophic failure of the device due to adhesion problems. Second, wear and friction of rubbing polysilicon components, eventually resulting in device failure due to friction, is an important reliability concern. Third, silicon is a brittle material below approximately 700K. Many MEMS applications require various types of deflection or high-speed rotation for their function. Such conditions can generate high tensile stresses. Crack initiation or growth would change the functionality of the component and could lead to its catastrophic failure.

Besides polysilicon, we are also investigating a material called "amorphous diamond" (aD) as a structural material for MEMS. This material is naturally hydrophobic, does not require special processing to obtain free devices, and exhibits very low wear rates. Stresses can also be reduced to low levels. Aside from processing techniques that are less advanced than those used for polysilicon, the only apparent disadvantage of amorphous diamond is that the deposition is not conformal around overhangs, making fabrication of hubs and flanges more difficult.

Use of MEMS materials requires a thorough knowledge about strength distributions, how etchants used for releasing the layers from sacrificial oxide layers affect strength, the types and sizes of flaws that cause failure, and the effect of stress concentrating features on device performance and reliability. Performance and reliability predictions also require an understanding of a material's failure mechanisms. Brittle materials such as silicon usually fail from surface flaws. Because the surface to volume ratio of microscopic components is much larger than for macrocomponents, surface quality due to both wet and dry etching procedures, and the influence of coatings used to minimize or prevent stiction problems, are likely to play a critical role in determining the strength and reliability of these devices.

Although various tests have been employed for determining the tensile[3] and bending strength[4,5] of relatively small-scale samples, it is critical to test polycrystalline samples whose sizes (several grains thick), microstructures, etching procedures, and flaw populations (e.g., dimples, etch release holes, and oxide cuts) are truly representative of the materials being used to fabricate MEMS devices. In this paper we will show how fracture strength can be measured for MEMS materials using a nanoindenter tool. Several generations of test structures were conceived to measure strength. Both proper test structure design and measurement method are important in obtaining accurate strength measurements. Fractography has been performed on the polysilicon and tungsten-coated polysilicon samples to identify the likely size and location of strength-limiting features.

SAMPLES AND STRENGTH TESTING TECHNIQUE

Pull-tab tensile samples designed to measure the fracture strength and elastic modulus of polysilicon were fabricated using Sandia's SUMMiT process. Figure 2a shows a first-generation polysilicon sample after it has been released from its sacrificial oxide support layer using a wet etchant. It has a freely moving pivot and a pull-tab. The pivot and pull-tab are connected by a nominally 2 μm wide, 2.5 μm thick ligament, whose length was varied from 15 to 1000 microns to test the effect of the gage length. As first-generation samples frequently failed outside the gage length, second-generation polysilicon samples were designed with a more robust pivot and larger gage-to-ring fillet (Fig. 2b). Two types of second-generation samples were tested, 98 samples made using two conventional release processes and 50 samples that had a post-release coating of tungsten.[6]

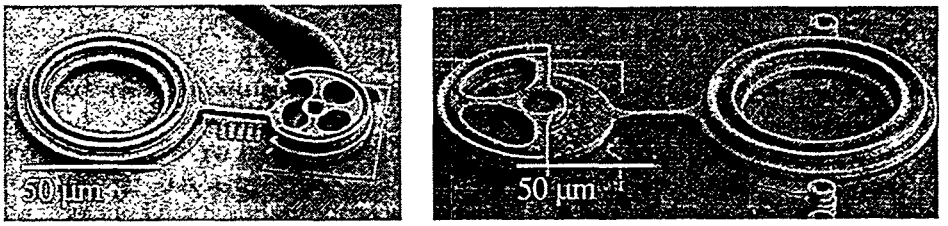

(a) (b)

Fig. 2. a) First generation tensile sample after release. b) Second generation sample with more robust pivot ring and larger radii in the gage length fillets.

Third-generation polysilicon samples were also fabricated with lengths of 15 to 1000 μm. They had the same pivot design and fillet radius as second-generation samples, but were nominally 4 μm wide, approximately twice as wide as the unnotched samples, and they included small notches made using a focused ion beam (FIB) (Fig. 3). The notches are intended to act as sharp cracks to allow the samples to be used for fracture toughness measurements.

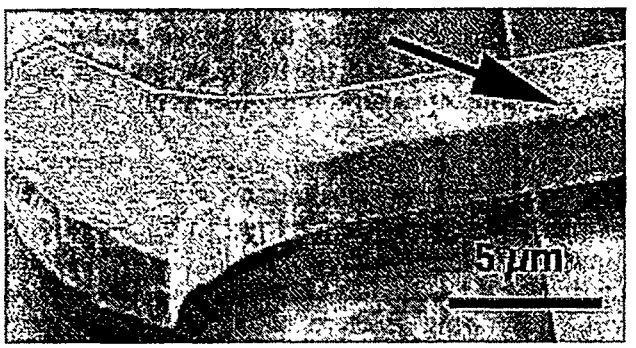

Fig. 3 Third generation sample with a notch (arrow) made using a focused ion beam (FIB).

Twenty-eight, single-layer amorphous diamond samples were fabricated with a pull-tab at one end and the other end fixed to the silicon die via a layer of SiO_2. The samples had the following nominal dimensions: thickness=1 μm thick; width=2.3 μm wide; and lengths=25, 100, and 500 μm.

This study used a tensile testing technique that utilizes the automated mode of a nanoindenter,* which provides the capability of testing 20-30 samples per day with little operator involvement. The test involves engaging the pull-tab end of the sample with a 35 μm diameter flat-tipped diamond on the nanoindentor (Fig. 4). The tip is centered within the pull-tab end of the tensile specimen and programmed to approach the silicon substrate until it senses surface contact. The tip then moves laterally to engage the pull-tab, while the normal force, lateral force, and displacement are recorded. The lateral displacement rate is 40 nm/s, which corresponds to strain rates of 2.7×10^{-3}/s and 4.0×10^{-5}/s for 15 and 1000 μm long samples, respectively. The force-displacement data are analyzed to calculate the stress-strain response. Load accuracy is ±50 μN and displacement accuracy is ±50 nm. Further details about the testing technique and data analysis can be found in References 3 and 7. The samples, which are trapped on the end of the indenter tip at the end of the test, are examined to identify the failure mode and origin.

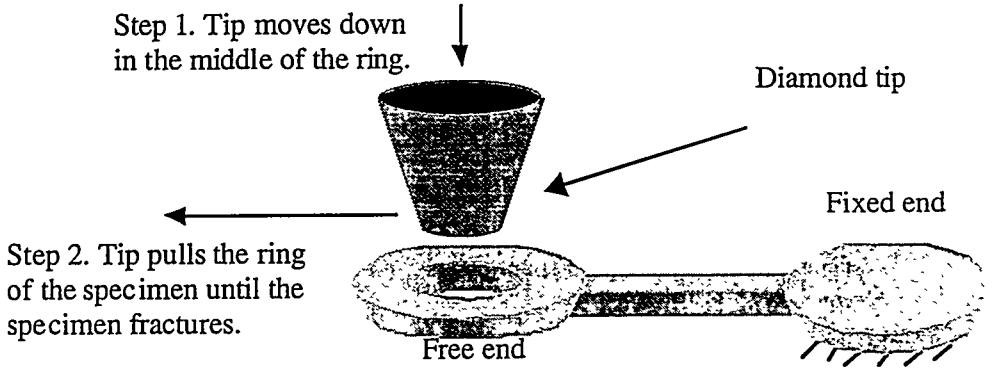

Fig. 4 Schematic of the test procedure.

RESULTS

The load deflection curves in Fig. 5 for four first-generation polysilicon samples show several distinct stages that correspond to different points within the loading sequence. The third region is the tensile loading segment of the test. The load deflection trace in this region is linear showing that the polycrystalline silicon samples deform in a linearly elastic manner up to the point of fracture.

The first set of tests was done on a group of 48 first-generation samples, 25 with 25 μm long gage lengths, and 23 with 15 μm long gage lengths. The cross-sectional dimensions are critical to the stress calculation and were measured to 0.1 μm in the SEM with a calibration standard. The samples measured, on average, 1.8 μm wide by 2.6 μm thick. The mean strength was 2.24±0.35 GPa. Fracture strengths grouped into three strength levels, which matched the three failure modes

* Nanoinstruments XP model.

observed in post-mortem examinations. The seven samples in the strongest group (σ_{mean}=2.77±0.04 GPa) failed in the gage section, the intermediate strength group failed at the gage section fillet, and the weakest group failed at a dimple. Figure 6 shows examples of each failure mode. There was no apparent correlation between the strengths and the gage length as the 15 micron long samples had an average strength of 2.24 ±0.37 GPa and the 25 micron long samples had a strength of 2.28±0.39 GPa.

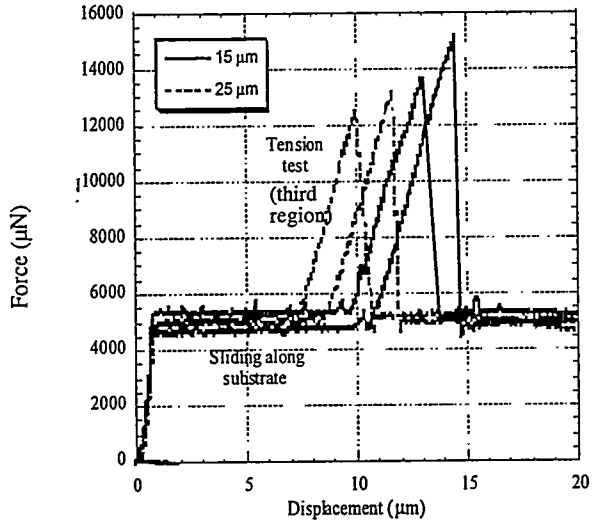

Fig. 5 The load deflection curves show several distinct stages that correspond to different points within the loading sequence.

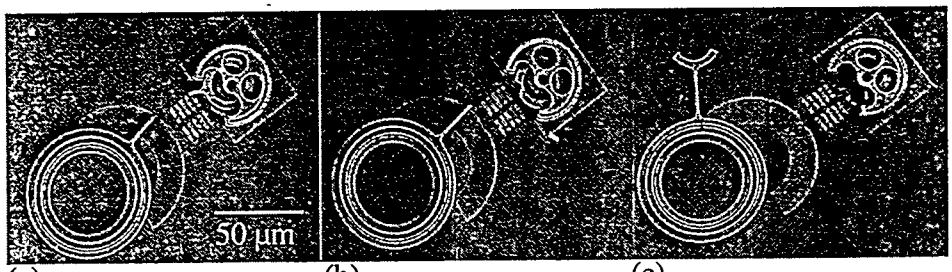

Fig. 6 Examples of each of the failure modes for first generation samples. (a) gage section (b) fillet (c) at dimple in pivot.

The Weibull plot shown in Fig. 7 for all first-generation polysilicon samples was constructed using the following failure probability (P_f) estimator, which works well for relatively small numbers of samples.[8]

$$P_f = (j-0.5)/n \qquad (1)$$

where j is the ranking of the sample and n is the number of samples.

The characteristic strength σ_o and Weibull modulus m, evaluated from the plot of ln ln $(1/(1-P_f))$ vs. ln (strength), are 2.4 GPa and 7.2, respectively.[9]

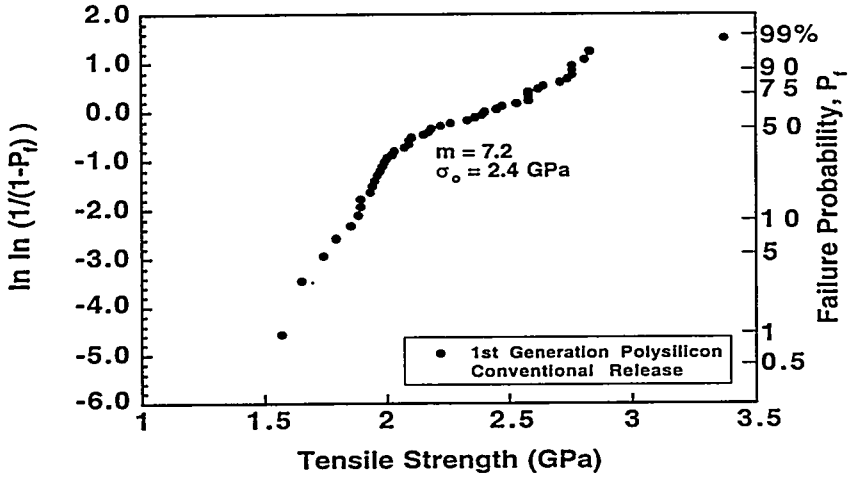

Fig. 7 Weibull plot of strengths from first generation polysilicon samples.

The second generation sample load-deflection results for different gage lengths allowed a graphical procedure to be used to determine a Young's modulus value of 170 GPa.[3] This is in good agreement with values for bulk polycrystalline silicon, which are 160-166 GPa. Texture measurements on our polysilicon show that it has a nearly random distribution of crystalline orientations,[10] so there should be no orientation effects.

The strength of the second-generation polysilicon samples, fabricated using two conventional release processes, is shown in Fig. 8 as a function of the gage length. The data for tungsten-coated samples fabricated using the same conventional release processes are also plotted in Fig. 8. Gage lengths of up to 1000 μm were used to determine whether there was a sample size/strength relationship as predicted by Weibull theory. A Weibull analysis was performed for the 98 conventionally released (CR) and 50 tungsten-coated (TC) samples. The strength data are shown in the Weibull plot in Fig. 9. The characteristic strength for the CR samples is 4.5 GPa (mean strength=4.3±0.6 GPa) and the m=8.4. The corresponding values for the TC samples are 3.0 GPa (mean strength=2.7±0.6 GPa) and m=5. The mean strength of amorphous diamond samples was 8.5±1.4 GPa.

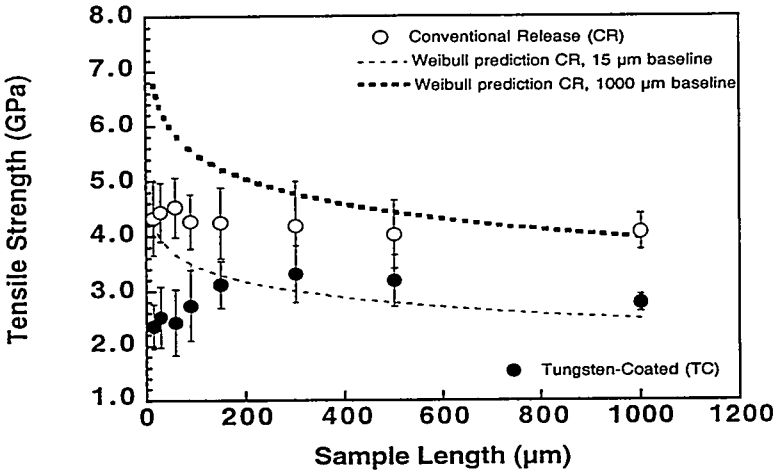

Fig. 8 Strengths of uncoated (open circles) and tungsten-coated (closed circles) polycrystalline silicon samples, processed using two conventional release processes, as a function of the gage length. Weibull size effect/strength predictions shown for uncoated conventionally released samples, using 15 and 1000 μm as the baseline strengths.

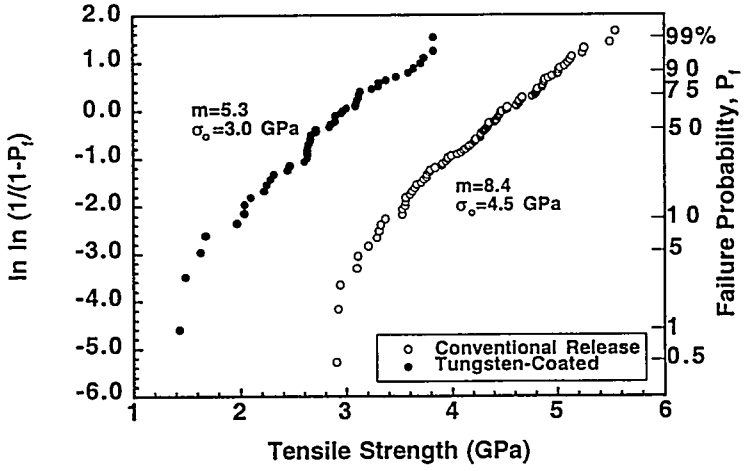

Fig. 9 A Weibull plot of strengths for 98 conventionally released and 50 tungsten coated polysilicon samples.

DISCUSSION

Second-generation polysilicon samples were much stronger than first-generation samples. Oddly, the strengths of first-generation samples that had failed in the gage were much lower than the strengths of second-generation samples that failed in the gage, suggesting that there may have been significant differences in sample processing or release. The strength of silicon materials has been shown to be very sensitive to the etchant and etching conditions. [11]

Previous tensile tests on polysilicon, with materials from another source, but with samples whose dimensions are comparable to those in these tests produced strengths of 1.20±0.15 GPa and 1.45±0.19 GPa, depending on sample size.[7] Tests using beam bending techniques reported strengths of 2.7 to 3.4 GPa.[7] Previous tests on single crystal silicon (<100> orientation) using biaxial flexure samples found Weibull characteristic strengths that ranged from 1.2 to 4.6 GPa for five different etching conditions.[12] The highest strengths corresponded to the etchants that produced the smoothest surfaces. The KOH etchant gave strengths (σ_0=3.4 GPa) and Weibull moduli (m=7-12) that were closest to those found for our second-generation conventionally released samples. Strength comparisons are shown in Table 1.

Table 1. Strength comparisons for MEMS materials.

Material and Fabrication Method	Dimensions w x t x L (μm unless noted otherwise)	Measurement Method	Fracture Strength (GPa)	Ref.
Silicon		Theoretical strength	19	Eq. 2
PolySi, SUMMiT, 1st gen.	1.8x2.5x15& 1.8x2.5x25	Direct uniaxial tension with nanoindenter	2.2±0.4	This study
PolySi, SUMMiT, 2nd gen.	1.8x2.5x(15 to 1000)	" "	4.3±0.6	This study
PolySi, SUMMiT, 2nd gen., W coating	1.8x2.5x(15 to 1000)	" "	2.7±0.6	This study
PolySi, SUMMiT, 2nd gen.	6x2.5x250 & 20x2.5x1000	Direct uniaxial tensionsample gripped with electrostatic force	2.9±0.4 2.8±0.4	13
<100> Silicon	t = 0.5 mm L=10 mm,	Biaxial flexure of square samples	1.2-4.6 *	12
Single crystal Si <110> loading and sample align.	w = 20-100 t = 3-5 L = 6 mm	Uniaxial tension of beam samples	0.6-1.2 **	11
Diamond		Theoretical strength	118	Eq. 2
Amorphous Diamond (aD)	2.3x1x500 & 2.3x1x1000	Direct uniaxial tension with nanoindenter	8.5±1.4	14

* Used five different surface conditions; two mechanical grinding conditions, and three etchants (KOH, DRIE, chemical polish).

** Used four etchants (KOH, EDP, TMAH, XeF_2)

A simple estimate of the theoretical cleavage strength σ_{th} of brittle materials can be made with the Young's modulus E, surface energy γ, and equilibrium interplaner spacing d_o.[15]

$$\sigma_{th} = (E\gamma/d_o)^{1/2} \qquad (2)$$

where E = 831 GPa for amorphous diamond
$2\gamma = 12$ J/m^2 for diamond
$d_o = 0.357$ nm for crystalline diamond

E = 170 GPa for polycrystalline Si
$2\gamma = 2.4$ J/m^2 for 111 single crystal Si
$d_o = 0.543$ nm for Si

This yields estimates of σ_{th} =19 GPa for silicon and 118 GPa for diamond. Thus the strengths measured in this study represent 10-20% of the theoretical strength of polysilicon and 7% of the theoretical strength of diamond.

The expected strength decrease for longer samples predicted by Weibull theory was not observed. A similar absence of a trend as a function of length was also obtained for the amorphous diamond specimens.[14] Figure 8 shows the Weibull prediction of the strength – volume effect for second-generation conventionally released polysilicon samples. The strength/volume relationship was calculated using the Weibull-based formula:

$$(\sigma_1/\sigma_2) = (V_2/V_1)^{1/m} \qquad (3)$$

where V = volume
σ = fracture strength
m = Weibull modulus

Sample thicknesses and widths are nominally the same and thus only the lengths were varied in this calculation. Both the strengths of the shortest and longest samples were used as baseline strengths. Clearly the observed trend of the strength being almost invariant with length does not match the expected trend for either baseline. It seems more likely that the strengths of the shortest samples are depressed relative to the expected value than that the longer samples are stronger than expected. There may be something in the sample fabrication that produces a more severe strength degradation effect for shorter samples. Further investigation is underway to understand this anomaly. In contrast to these results, others have observed the expected trend, whereby the strength of polysilicon increased as sample length decreased.[16]

Failure origin size estimates can be used to help identify processing defects that could be eliminated to improve the strength and reliability of MEMS devices.

The strength can be used along with the fracture toughness to estimate the size of strength-limiting defects using the Griffith relationship:

$$K_{IC} = \sigma_f Y(\pi c)^{1/2} \quad (4)$$

where K_{IC} =fracture toughness

σ_f =failure stress

c = failure origin size

Y = geometrical loading factor (used 1.12)

Compression-loaded double cantilever beam (DCB) samples were used to measure the fracture toughness of MEMS-scale single crystal silicon samples.[15] A mean value of 1.3 MPa$\sqrt{m}$ was determined. Chen and Leipold measured the fracture toughness of single crystal silicon for different planes and found that an average value of ~1 MPa$\sqrt{m}$ was appropriate.[17] Because failure originates within single grains (grain size typically <0.5 μm), the single crystal fracture toughness of 1 MPa$\sqrt{m}$ was used in Eq. 4 to estimate the flaw size. Using the strengths obtained for the first (2.2 GPa) and second-generation samples (2.7 and 4.3 GPa,) the critical flaws are estimated to be in the range of 14-44 nm. This is much smaller than the size of the structures and features that are typical of a MEMS device (Fig. 1) and represents approximately 1-2% of the sample cross section dimensions.

Tests of single crystal silicon samples with different orientations have shown that strength is very dependent on the orientation.[12] Because the failure origins in this study are much smaller than the polysilicon grains, the orientation of the grain in which failure originates is likely to have an important effect on the strength. Because strength is a function of the fracture toughness K_{IC} (Eq. 4), variability in K_{IC} due to orientation or other effects is likely to affect the strength variability. The Weibull modulus and characteristic value of the toughness were calculated for the single crystal fracture toughness data in the study by Fitzgerald et al.[19] A characteristic toughness of 1.42 MPa$\sqrt{m}$ and an m=4.8 were obtained. Thus the high variability in the fracture toughness, as demonstrated even for a single orientation of Si, may be a major contributor to the strength variability, and help explain why the Weibull moduli for these materials are low, even relative to other brittle materials such as structural ceramics (m=7-15).[18]

Figure 10 shows an SEM photo of the fracture surface of a tungsten-coated sample. The approximate position of the failure origin at the original surface can be determined from the fracture surface hackle markings. Figure 11 shows a TEM cross section of the top layer of a W-coated sample. There are particle intrusions at the W-polysilicon interface that are much smaller than the silicon grain size. Their size is consistent with the failure origin size estimate from Eq. 4. These particles may be responsible for the degraded strength (from 4.3 to 2.7 GPa) of the W-coated samples relative to uncoated samples from the same production run.

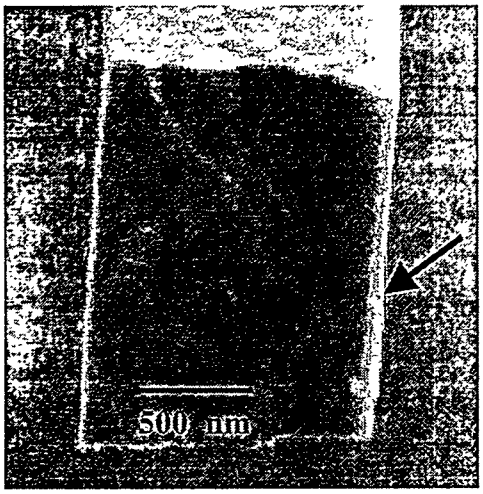

Fig. 10 The fracture surface of a tungsten-coated sample. The approximate position of the failure origin (arrow) can be determined from the fracture surface markings.

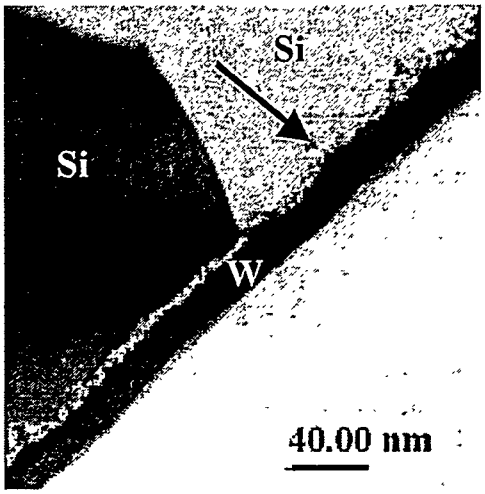

Fig. 11 A TEM cross section of particle intrusions (arrow) at the W-polysilicon interface in a W-coated sample.

Figure 12 shows the fracture surface of a third-generation polysilicon sample, for which we were unable to obtain the fracture load. Based on the appearance and location of the fracture surface features, failure initiated at the external surface. The fracture branching boundary radius r_B and the single crystal silicon crack branching constant K_B=2 MPa$\sqrt{m}$ [20] can be used in a formulation similar to Eq. 4 (where σ_f =failure stress and Y=geometrical constant) to estimate a failure stress of 2.1 GPa. This value is consistent with, but slightly lower than strengths measured for similar samples.

$$\sigma_f Y r_B^{1/2} = \text{constant} = K_B \qquad (5)$$

Third-generation samples with focused ion beam (FIB) notches frequently did not fail from the notch as shown in Fig. 3. These results suggest that the notch is not serving as a flaw that produces a high stress concentration. The sample in Fig. 3 appears to have failed at a dimple in the pivot, which in turn suggests that it has a high stress concentration associated with it.

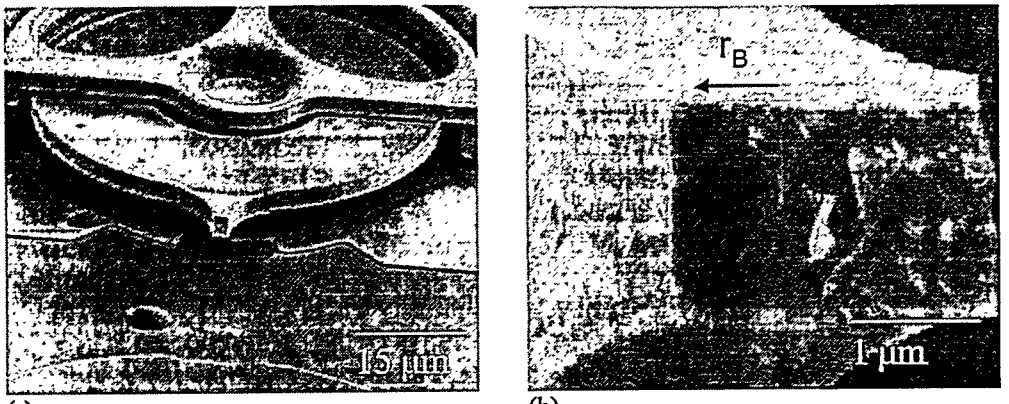

(a) (b)

Fig. 12 (a) Low magnification view of fractured polysilicon sample. (b) Higher magnification showing fracture branching boundary (r_B) used to estimate fracture strength.

SUMMARY AND CONCLUSIONS

The scatter in the strengths of polysilicon and amorphous diamond samples and the sensitivity of the strengths to the etching process and geometry clearly indicate the need to use a probabilistic design approach when using these materials for MEMS applications. However, in contrast to results for most brittle materials and to Weibull theory predictions, the strengths of these materials do not appear to depend on the size of the sample. Further study of this effect is underway. The difference between the strengths measured for the first and second-generation samples, and between the conventionally released samples and tungsten-coated samples, also highlights the need to understand and control the processing and to characterize strength distributions for different processing routes. The strength levels imply flaw dimensions of 14-44 nm, smaller than the silicon grains, and much smaller than the geometrical features that are typical of MEMS devices.

ACKNOWLEDGMENTS

The staff of the Microelectronics Development Laboratory at Sandia National Laboratories is gratefully acknowledged for their fabrication work. Thanks to M. De Boer for his thoughtful review and input to the paper. Thanks to B. McKenzie and P. Kotula for the microstructural analyses. Sandia is a multiprogram laboratory operated by Sandia Corporation, a Lockheed Martin Company, for the United States Department of Energy under Contract DE-ACO4-94AL85000.

REFERENCES

1. Intelligent Micromachine Initiative, Sandia National Laboratories, http://www.mdl.sandia.gov/Micromachine, 2000.

2. J. J. Sniegowski and M. P. de Boer, "IC-Compatible Polysilicon Surface Micromachining," Annu. Rev. Mater. Sci, No. 30, pp. 299-333 (2000).

3. D. A. LaVan and T. E. Buchheit, "Testing of Critical Features of Polysilicon MEMS," to be published in the proceedings of the 1999 MRS Fall Meeting, Boston, MA, 1999.

4. J. Koskinen, J. E. Steinwall, R. Soave, and H. H. Johnson, "Microtensile Testing of Free-Standing Polysilicon Fibers of Various Grain Sizes," J.

Micromech. Microeng., 3, pp. 13-17 (1993).

5. S. B. Brown, G. Povirk, and J. Connally, "Measurement of Slow Crack Growth in Silicon and Nickel Micromechanical Devices," pp. 99-104 in Electro Mechanical Systems -MEMS, IEEE Proc. (1993).

6. S. S. Mani, J. G. Fleming, J. J. Sniegowski, M. P. de Boer, L. W. Irwin, J. A. Walraven, D. M. Tanner, D. A. LaVan, "Selective W for Coating and Releasing MEMS Devices," Symposium MM, Materials Science of Microelectromechanical Systems (MEMS) II, Proc. of the MRS Fall Meeting, Boston, Dec. 1-3, 1999.

7. D. A. LaVan and T. E. Buchheit, "Reliability Testing of Polysilicon for MEMS Devices," to be published in the proceedings of the conference on Micro/Nanotechnology for Space Applications, Pasadena, CA, Apr. 1999.

8. J. D. Sullivan and P. H. Lauzon, "Experimental Probability Estimators for Weibull Plots," J. Mater. Sci. Lett., Vol. 5, pp. 1245-1247 (1986).

9. W. Weibull, "A Statistical Theory of the Strength of Materials," Proc. Royal Swedish Institute Engineering Research, No. 151, pp. 1-45 (1939).

10. D. A. LaVan, T. E. Buchheit, and J. R. Michael, "Grain Structure and Texture of Individual Polysilicon Layers for MEMS," poster in Symposium MM, Materials Science of Microelectromechanical Systems (MEMS) Devices II, MRS Fall Meeting, Boston, Nov. 1999.

11. T. Yi, L. Li, and C.J. Kim, "Microscale Material Testing of Single Crystalline Silicon: Process Effects on Surface Morphology and Tensile Strength," Sensors and Actuators, 83, pp. 172-178 (2000).

12. K-S. Chen, A. Ayon, and S. M. Spearing, "Controlling and Testing the Fracture Strength of Silicon on the Mesoscale," J. Am. Ceram. Soc., 83 [6] 1476-84 (2000).

13. D. A. LaVan, T. Tsuchiya, W. N. Sharpe, and O. L. Warren, "Cross Comparison of Direct Tensile Testing Techniques on SUMMiT Polysilicon Films," to be presented at the ASTM Symposium on Mechanical Properties of Structural Films, Orlando, FL, Nov. 15-16, 2000.

14. D. A. LaVan, R. J. Hohlfelder, J. P. Sullivan, T. A. Friedmann, M. Mitchell, and C. I. H. Ashby, "Tensile Properties of Amorphous Diamond Films," Symposium U, Amorphous and Nanostructured Carbon, to be published in the proceedings of the 1999 MRS Fall Meeting, Boston, Dec. 1-3, 1999.

15. D. J. Green, An Introduction to the Mechanical Properties of Ceramics, p. 211, Cambridge University Press, 1998.

16. T. Yi and C-J. Kim, "Measurement of Mechanical Properties for MEMS Materials," Meas. Sci. Tech., 10, pp. 706-716 (1999).

17. P. Chen and M. H. Leipold, "Fracture Toughness of Silicon," Am. Ceram. Soc. Bull., 59 pp. 469-72 (1980).

18. A. F. McClean, "An Overview of the Ceramic Design Process," pp. 677-689 in Vol. 4 Engineered Materials Handbook, Ceramics and Glasses, ASM International, 1991.

19. A. M. Fitzgerald, R. H. Dauskardt, and T. W. Kenny, "Fracture Toughness and Crack Growth Phenomena of Plasma-Etched Single Crystal Silicon," Sensors and Actuators, 83, pp. 194-199 (2000).

20. Y. L. Tsai and J. J. Mecholsky, Jr., "Fracture Mechanics Description of Fracture Mirror Formation in Single Crystals," Intl. J. Frac., 57, 167-182, (1992).